



This is a repository copy of *Characteristics of C-4 photosynthesis in stems and petioles of C-3 flowering plants*.

White Rose Research Online URL for this paper:  
<http://eprints.whiterose.ac.uk/113/>

---

**Article:**

Hibberd, J.M. and Quick, W.P. (2002) Characteristics of C-4 photosynthesis in stems and petioles of C-3 flowering plants. *Nature*, 415 (6870). pp. 451-454. ISSN 0028-0836

<https://doi.org/10.1038/415451a>

---

**Reuse**

Unless indicated otherwise, fulltext items are protected by copyright with all rights reserved. The copyright exception in section 29 of the Copyright, Designs and Patents Act 1988 allows the making of a single copy solely for the purpose of non-commercial research or private study within the limits of fair dealing. The publisher or other rights-holder may allow further reproduction and re-use of this version - refer to the White Rose Research Online record for this item. Where records identify the publisher as the copyright holder, users can verify any specific terms of use on the publisher's website.

**Takedown**

If you consider content in White Rose Research Online to be in breach of UK law, please notify us by emailing [eprints@whiterose.ac.uk](mailto:eprints@whiterose.ac.uk) including the URL of the record and the reason for the withdrawal request.



[eprints@whiterose.ac.uk](mailto:eprints@whiterose.ac.uk)  
<https://eprints.whiterose.ac.uk/>

# Characteristics of C<sub>4</sub> photosynthesis in stems and petioles of C<sub>3</sub> flowering plants

Julian M. Hibberd\* & W. Paul Quick†

\* Department of Plant Sciences, University of Cambridge, Downing Street, Cambridge CB2 3EA, UK

† Robert Hill Institute, Department of Animal and Plant Sciences, University of Sheffield, Western Bank, Sheffield S10 2TN, UK

Most plants are known as C<sub>3</sub> plants because the first product of photosynthetic CO<sub>2</sub> fixation is a three-carbon compound<sup>1</sup>. C<sub>4</sub> plants, which use an alternative pathway in which the first product is a four-carbon compound, have evolved independently many times and are found in at least 18 families<sup>2,3</sup>. In addition to differences in their biochemistry, photosynthetic organs of C<sub>4</sub> plants show alterations in their anatomy and ultrastructure<sup>4</sup>. Little is known about whether the biochemical or anatomical characteristics of C<sub>4</sub> photosynthesis evolved first. Here we report that tobacco, a typical C<sub>3</sub> plant, shows characteristics of C<sub>4</sub> photosynthesis in cells of stems and petioles that surround the xylem and phloem, and that these cells are supplied with carbon for photosynthesis from the vascular system and not from stomata. These photosynthetic cells possess high activities of enzymes characteristic of C<sub>4</sub> photosynthesis, which allow the decarboxylation of four-carbon organic acids from the xylem

and phloem, thus releasing CO<sub>2</sub> for photosynthesis. These biochemical characteristics of C<sub>4</sub> photosynthesis in cells around the vascular bundles of stems of C<sub>3</sub> plants might explain why C<sub>4</sub> photosynthesis has evolved independently many times.

Photosynthesis forms the basis on which all ecosystems on Earth function. The biochemical pathways of photosynthesis are highly conserved. Most plants are C<sub>3</sub> plants, in which the first product of photosynthesis is the three-carbon compound phosphoglyceric acid<sup>1</sup>. A second biochemical pathway that allows the concentration of CO<sub>2</sub> in leaves has evolved in C<sub>4</sub> plants, which initially fix inorganic carbon in mesophyll cells into the four-carbon compound oxaloacetic acid. In C<sub>4</sub> plants, oxaloacetate is converted into malate or aspartate, which then diffuses into bundle sheath cells that surround the vascular bundles where decarboxylation supplies high concentrations of CO<sub>2</sub> to Rubisco. The C<sub>4</sub> pathway is thought to have evolved independently 31 times in 18 taxonomic families of angiosperms, and occurs in 8,000 to 10,000 species<sup>2,3</sup>. The presence of C<sub>4</sub> photosynthesis in unicellular algae has also been reported<sup>5</sup>. In higher plants the C<sub>4</sub> pathway involves both biochemical and anatomical modifications, but it is not clear which of these modifications evolved first<sup>2,6</sup>.

Some plants that possess characteristics of both C<sub>3</sub> and C<sub>4</sub> plants have been classified as C<sub>3</sub>-C<sub>4</sub> intermediates<sup>7</sup>, and these may represent transitional stages in the evolution of C<sub>4</sub> photosynthesis from C<sub>3</sub> photosynthesis. In C<sub>3</sub>-C<sub>4</sub> intermediates, a photorespiratory cycle has been reported to shunt the precursors of photorespiratory CO<sub>2</sub> from the mesophyll to the bundle sheath<sup>8,9</sup>; in addition, it has been proposed that a pathway that recaptures CO<sub>2</sub> lost during photorespiration and that concentrates CO<sub>2</sub> around Rubisco in bundle sheath cells represents the first step in C<sub>4</sub> evolution<sup>6,7</sup>.

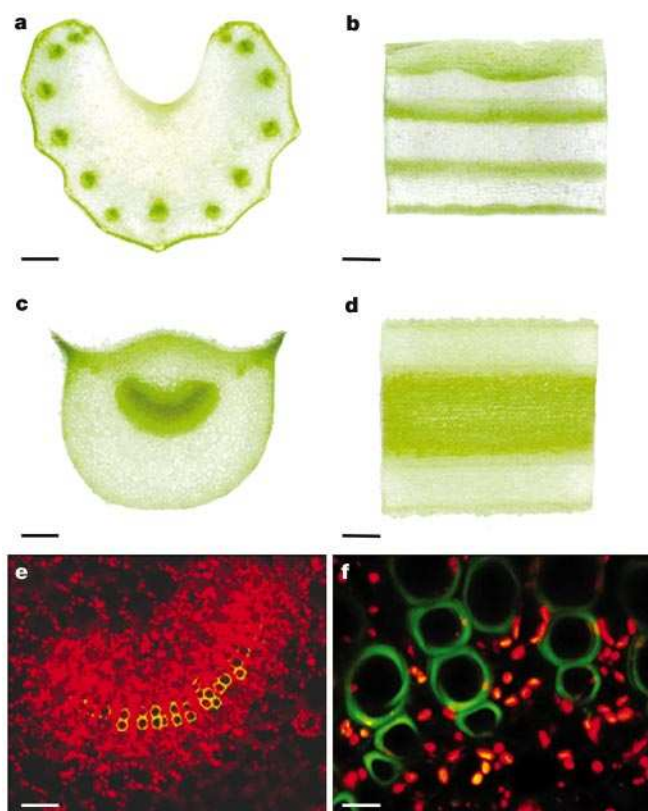


**Figure 1** Distribution of chlorophyll in petioles of celery and tobacco. **a**, Transverse section of celery. **b**, Longitudinal section of celery. **c**, Transverse section of tobacco. **d**, Longitudinal section of tobacco. **e**, Confocal laser scanning microscope image showing chlorophyll fluorescence around the vascular system. **f**, Confocal laser scanning microscope image showing chloroplasts (red) in between the xylem vessels (green). Scale bars, 2.6 mm (**a**, **b**); 1.0 mm (**c**); 1.1 mm (**d**); 175 μm (**e**); 25 μm (**f**).

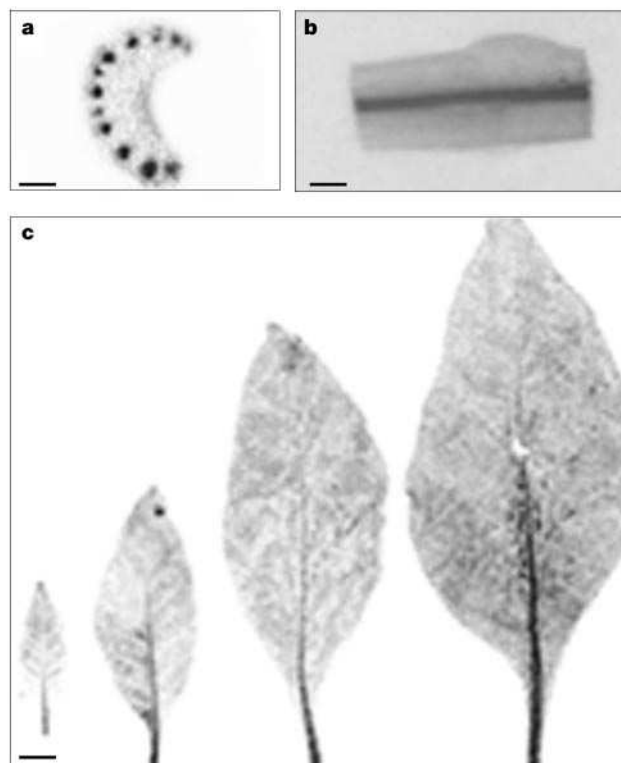


**Figure 2** Incorporation of <sup>14</sup>C into insoluble material in cells around the vascular system of celery and tobacco. **a**, Transverse section of celery after [<sup>14</sup>C]NaHCO<sub>3</sub> was fed to the xylem stream. Scale bar, 4.5 mm. **b**, Longitudinal section of tobacco showing <sup>14</sup>C fixed into starch after [<sup>14</sup>C]NaHCO<sub>3</sub> was supplied to the xylem stream. Scale bar, 2.3 mm. **c**, Leaves from tobacco show that when malate with a <sup>14</sup>C label on the C4 position is supplied to the xylem stream, <sup>14</sup>C is fixed in cells surrounding the vascular system. Young to old leaves are shown left to right. Scale bar, 14 mm.

Three separate biochemical pathways have evolved to decarboxylate the C<sub>4</sub> acid in the bundle sheath cells and thus supply Rubisco with CO<sub>2</sub>; however, we know little about how these different pathways evolved. In addition to the limited number of biochemical pathways that allow fixation of inorganic carbon in flowering plants, there are few exceptions to the normal route that CO<sub>2</sub> takes to reach the sites of fixation. The pathway of CO<sub>2</sub> moving into a plant through stomata is almost universal in vascular land plants. Notable exceptions are submerged aquatic members of the Isoetaceae that do not produce stomata on submerged leaves and vary in their ability to form stomata on aerial leaves<sup>10</sup>. For example, the CAM (crassulacean acid metabolism) plant *Stylites andicola*, which is a rare ally of ferns, does not possess stomata and CO<sub>2</sub> is transferred to the leaves through its root system<sup>11</sup>. In *Cuscuta reflexa*, a parasitic plant in which stomata have become modified into extrafloral nectaries, CO<sub>2</sub> fixed in photosynthesis is derived internally from respiration<sup>12</sup>.

We studied a group of photosynthetic cells surrounding the vascular tissue of stems and petioles in tobacco that continue their association with vascular bundles well into the leaf tissue. Even in C<sub>3</sub> plants, cells around the veins are termed 'bundle sheath' cells<sup>13,14</sup>. Although these photosynthetic cells are evident to the naked eye in plants such as celery (Fig. 1a, b), they have not been included in classifications of stem photosynthesis to date<sup>15</sup>. In transverse and longitudinal sections of celery (Fig. 1a, b) and tobacco (Fig. 1c–e), the most intense regions of chlorophyll accumulation are associated directly with internal vascular structures. Chlorophyll is found preferentially surrounding the xylem and the phloem of the vascular bundles (Fig. 1e), and chlorophyll fluorescence from the chloroplasts of cells directly between the xylem vessels can be observed (Fig. 1f). In fact, species from 30 different families that we have so far examined contain chlorophyll around the phloem and xylem vessels (data not shown).

In contrast to CO<sub>2</sub> movement to all other photosynthetic cells in flowering plants, CO<sub>2</sub> diffusion from stomata to the photosynthetic cells surrounding the vascular bundles is likely to be slow as there are relatively few stomata, many layers of surrounding cells and very few intercellular air spaces. This lack of air spaces between cells of the

vascular tissue has been previously noted and proposed to reduce diffusion of oxygen to cells that would be prone to oxidative stress<sup>16</sup>. But the photosynthetic cells that we observed have the potential to generate active oxygen species in cells close to the vascular system. As these photosynthetic cells are not close to stomata but are close to the xylem vessels, we tested whether they fix inorganic carbon supplied from the xylem stream.

Inorganic carbon supplied to roots and stems of tobacco and celery as [<sup>14</sup>C]NaHCO<sub>3</sub> led to accumulation of <sup>14</sup>C in insoluble material, most notably starch, in cells associated with the vasculature (Fig. 2a, b). Supplying [<sup>14</sup>C]glucose to roots (which is taken up by the roots and used in respiration to produce <sup>14</sup>CO<sub>2</sub>) led to <sup>14</sup>C in the xylem stream and the same distribution of isotope around the vascular bundles (data not shown). These data show that inorganic carbon surrounding roots can be taken up and fixed by cells around the xylem, and also that sugars used in respiration in roots give rise to CO<sub>2</sub> that moves into xylem vessels and is then fixed by cells surrounding the xylem. The concentration of CO<sub>2</sub> in the xylem sap is dependent on pH, and considerably higher than that in the air<sup>17</sup>. Supplying inorganic carbon to the roots of plants has been shown to enhance plant growth and productivity<sup>18,19</sup>, although it should be noted that the growth enhancement is not completely due to fixation of the additional inorganic carbon supply<sup>19,20</sup>.

The xylem stream of plants often contains organic acids<sup>21,22</sup>, and the malate found in both phloem and xylem may have a role as a biochemical pH regulator to balance acid and base movement through the plant<sup>22,23</sup>. We tested whether malate supplied to the transpiration stream would be decarboxylated, and the released CO<sub>2</sub> subsequently re-fixed photosynthetically by the cells surrounding the xylem vessels. Feeding malate labelled with <sup>14</sup>C in the C4 position (this is the carbon atom that is released during the decarboxylation process) to the xylem stream led to the fixation of <sup>14</sup>C in the veins of the petioles and stems of tobacco (Fig. 2c). Concentrations of malate in the xylem sap of tobacco plants decreased with increasing distances from the base of the plant (0.23 mM at the base to 0.02 mM in expanded leaves)<sup>24</sup>. Changes in the concentration of malate in the xylem have implications for the acid–base balance of the shoot<sup>22</sup>, and therefore merit further

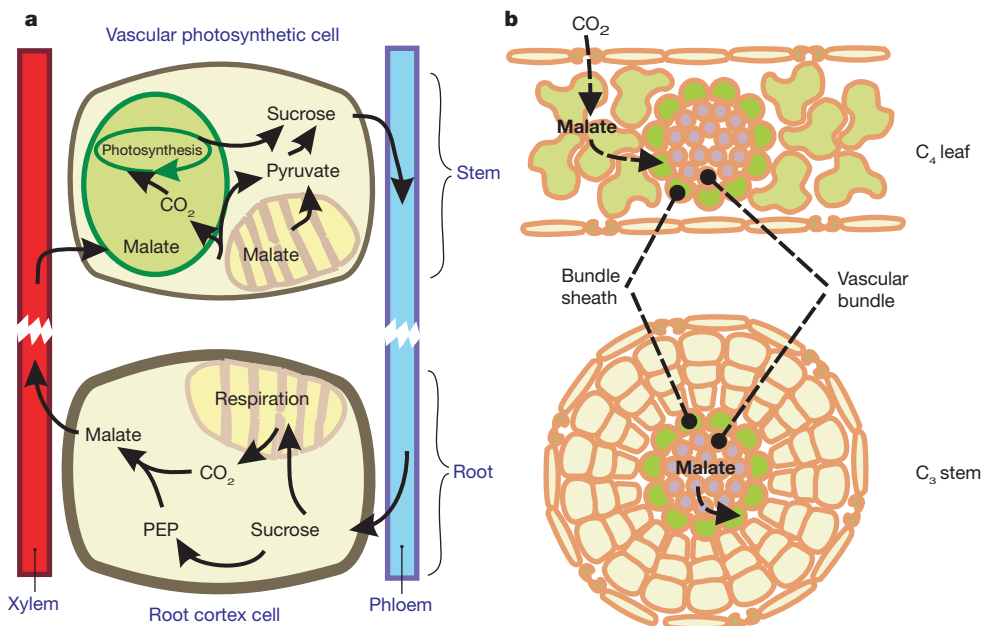


**Figure 3** Photosynthesis around the veins of C<sub>3</sub> and C<sub>4</sub> plants. **a**, Model for the role of photosynthesis around the vascular system of stems and petioles of the C<sub>3</sub> plant tobacco. CO<sub>2</sub> is supplied from the soil, from respiration in roots or from malate that is produced in the root; either CO<sub>2</sub> or malate moves into the xylem stream, which supplies photosynthetic

cells lining the vascular system in stems and petioles. **b**, Comparison of the supply of malate to photosynthetic cells in a C<sub>4</sub> leaf and that to photosynthetic cells lining the vascular system in a C<sub>3</sub> stem. Both sets of cells that line the vascular system possess high activities of enzymes that can decarboxylate C<sub>4</sub> organic acids.

investigation. We conclude that these photosynthetic vascular cells scrub the xylem of malate, because the <sup>14</sup>C label was restricted to the petiole and basal regions of all leaves in a plant (Fig. 2c).

When the plants were left for 24 h (after supplying the transpiration stream with radiolabelled malate for 1 h), we found that <sup>14</sup>C no longer remained within the vascular tissues but was transferred to young developing leaves. Placing plants in darkness to close the stomata showed that this process was independent of the transpiration stream. We therefore conclude from this indirect data that sucrose produced from these cells around the vascular bundles is loaded into the phloem and translocated to growing apices. These data indicate that photosynthetic cells around the vasculature make use of organic acids present in the xylem of tobacco.

The decarboxylation of malate in cells around the veins of petioles and stems is reminiscent of the decarboxylation of organic acids in the bundle sheath of C<sub>4</sub> plants—that is, the cells that surround the vascular bundles of leaves. To test whether decarboxylation enzymes are specifically and preferentially expressed in cells around the vascular bundles in the stem of tobacco, we determined the activity of three decarboxylation enzymes—nicotinamide adenine dinucleotide (NAD)-malic, NADP-malic and phosphoenolpyruvate carboxykinase (PEPCK)—indicative of the three C<sub>4</sub> subtypes, and compared their activity in these cells with that in the leaf lamina. In cells surrounding the xylem and phloem of tobacco, the activity of NAD-malic enzyme (NAD-ME) was 13-fold higher than in the leaf, and the activity of NADP-malic enzyme (NADP-ME) and PEPCK were both 9-fold higher than in the leaf (Table 1). The activities of these decarboxylation enzymes far exceeds typical values obtained from C<sub>3</sub> plants and approaches activities expected in the bundle sheath of C<sub>4</sub> plants<sup>25,26</sup>. These data indicate that in tobacco, a C<sub>3</sub> plant, similar biochemical attributes to those needed in C<sub>4</sub> photosynthesis are associated with photosynthesis around the vascular system of stems and petioles.

Because these enzymes are expressed highly and specifically in these cells, the correct regulatory elements controlling gene expression must be present. In agreement with our assays of enzyme activity, when present in tobacco the promoter of a gene coding NADP-ME from bean directs high and specific expression of the enzyme in cells surrounding the vascular tissue of stems<sup>27</sup>. Notably, in the *Arabidopsis* genome the genes that code these decarboxylases are members of gene families that would allow the differential regulation and tissue-specific expression of certain members of each family. The vascular system may be regarded as taking the place of the mesophyll cells of a C<sub>4</sub> plant by supplying the surrounding photosynthetic cells with malate. The malate is then decarboxylated, and thus part of the C<sub>4</sub> cycle is operating in C<sub>3</sub> plants.

We also measured high activities of phosphoenol pyruvate orthophosphate dikinase (PPDK; this regenerates PEP from pyruvate in C<sub>4</sub> plants) in cells around the vascular system of tobacco petioles (Table 1). The role that the decarboxylases have in cells around the vascular system is not certain. It is possible that by controlling the concentration of malate, they are involved in controlling the pH of the xylem<sup>22</sup>. In addition, their high activity and the production of PEP through PPDK would allow for high provision of carbon skeletons into the shikimate pathway and thus

lignin synthesis in exactly the cells where lignin is incorporated into cell walls of the xylem vessels at high rates.

From these data we propose the following scheme. In C<sub>3</sub> plants, photosynthetic cells surrounding the vascular system are supplied with either malate or CO<sub>2</sub> from the xylem vessels (Fig. 3a). CO<sub>2</sub> can be supplied from root respiration, or enter the roots from the soil. Malate is produced from PEP because of the presence of phosphoenolpyruvate carboxylase in roots<sup>18,28,29</sup>. Malate is then decarboxylated by cells bordering the vascular system in the stems of C<sub>3</sub> plants, and the CO<sub>2</sub> is used in photosynthesis to produce carbohydrates including sucrose and starch (Fig. 3a). The sucrose that is produced can be either used locally to fuel metabolism or loaded into the phloem and translocated to growing regions of the plant. When compared to the system that operates in C<sub>4</sub> plants, there are striking parallels (Fig. 3b). Bundle sheath cells of C<sub>4</sub> plants are photosynthetic, lie adjacent to vascular tissues, and possess high activities of enzymes that release CO<sub>2</sub> from malate. These key attributes of C<sub>4</sub> photosynthesis are also characteristics of the photosynthetic cells that surround the vascular bundle in C<sub>3</sub> plant stems and petioles that we have identified here. The main difference is the source of malate: in C<sub>4</sub> plants, malate is provided by adjacent mesophyll cells; in C<sub>3</sub> stems and petioles, malate is derived from the respiratory activity of distant heterotrophic tissues and transported through the vasculature to photosynthetic cells surrounding the vascular system.

We propose that the arrangement of photosynthetic cells around vascular bundles of C<sub>3</sub> stems is a more spatially separated version of the C<sub>4</sub> photosynthetic pathway. Furthermore, the presence of the correct biochemical pathways in cells adjacent to the vascular bundles in the stems and leaf veins of C<sub>3</sub> plants indicates that essential biochemical components and the regulatory elements controlling the cell-specific gene expression required for C<sub>4</sub> photosynthesis are already present in C<sub>3</sub> plants; thus, fewer modifications are needed for C<sub>4</sub> photosynthesis to evolve. The promoter of an NADP-ME gene from bean has been shown to direct expression in cells around the vascular system<sup>27</sup>. The existence of such a similar pathway in C<sub>3</sub> plants provides a simple explanation for the polyphyletic evolution of C<sub>4</sub> photosynthesis. □

## Methods

### Plants and microscopy

Tobacco plants were grown under natural light in a greenhouse with supplementary lighting provided by metal halide bulbs supplying 250 μmol photons m<sup>-2</sup> s<sup>-1</sup>. Plants were used during vegetative growth between 40 and 60 days after planting. We collected and analysed xylem sap as described<sup>24</sup>. We cut sections for optical and confocal laser scanning microscopy manually with a razor blade. Images of chlorophyll fluorescence were taken using the TRITC channel of a Leica TCS confocal microscope.

### <sup>14</sup>C labelling and enzyme assays

We fed 1 mM [<sup>14</sup>C]NaHCO<sub>3</sub> (specific activity 155 MBq mmol<sup>-1</sup>), 0.1 mM <sup>14</sup>C universally labelled glucose (74 MBq mmol<sup>-1</sup>) or 0.2 mM malate (80 MBq mmol<sup>-1</sup>) labelled in the C4 position to the roots or stems of tobacco grown hydroponically, and to the stems of celery for 40 min in the light. Plants were left for 30 min, flash frozen, and heated in 70% ethanol to remove soluble sugars; sections were then exposed to X-ray film. We conducted enzyme assays on either leaf lamina of tobacco or the veins of tobacco petioles separated from the cortex manually with a razor blade; results are expressed per unit chlorophyll<sup>25,30</sup>.

Received 13 September; accepted 21 November 2001.

**Table 1 Activities of decarboxylation enzymes and PPDK**

	NAD-ME activity (μmol min <sup>-1</sup> per mg Chl)	NADP-ME activity (μmol min <sup>-1</sup> per mg Chl)	PEPCK activity (μmol min <sup>-1</sup> per mg Chl)	PPDK activity (μmol min <sup>-1</sup> per mg Chl)
Leaf tissue	0.25 ± 0.03	0.78 ± 0.08	0.003 ± 0.0007	0.30 ± 0.05
Vein tissue	3.15 ± 0.22	6.82 ± 1.07	0.028 ± 0.009	5.33 ± 1.06
Relative enrichment (vein/leaf)	13-fold	9-fold	9-fold	18-fold

These enzymes are used by C<sub>4</sub> plants and are here measured in tobacco. Data shown are means ± s.e. (n = 8–13). Chl, chlorophyll.

- Calvin, M. et al. Carbon dioxide assimilation in plants. *Symp. Soc. Exp. Biol.* 5, 284–305 (1951).
- Moore, P. D. Evolution of photosynthetic pathways in flowering plants. *Nature* 310, 696 (1982).
- Sage, R. F., Li, M. & Monson, R. K. in *C<sub>4</sub> Plant Biology* (eds Sage, R. F. & Monson, R. K.) 551–584 (Academic, San Diego, 1999).
- Hatch, M. D. C<sub>4</sub> photosynthesis; a unique blend of modified biochemistry, anatomy and ultra-structure. *Biochem. Biophys. Acta* 895, 81–106 (1987).
- Reinfelder, J. R., Kraepiel, A. M. L. & Morel, F. M. Unicellular C<sub>4</sub> photosynthesis in a marine diatom. *Nature* 407, 996–999 (2000).
- Monson, R. K. in *C<sub>4</sub> Plant Biology* (eds Sage R. F. & Monson, R. K.) 377–410 (Academic, San Diego, 1999).
- Rawsthorne, S. C<sub>3</sub>–C<sub>4</sub> intermediate photosynthesis: linking physiology to gene expression. *Plant J.* 2, 267–274 (1992).
- Rawsthorne, S., Hylton, C. M., Smith, A. M. & Woolhouse, H. W. Photorespiratory and immunogold localization of photorespiratory enzymes in leaves of C<sub>3</sub> and C<sub>3</sub>–C<sub>4</sub> intermediate species of *Moricondia*. *Planta* 173, 298–308 (1988).



9. Rawsthorne, S., Hylton, C. M., Smith, A. M. & Woolhouse, H. W. Distribution of photorespiratory enzymes between bundle sheath and mesophyll cells in leaves of the C<sub>3</sub>-C<sub>4</sub> intermediate species *Moricondia arvensis* (L.) DC. *Planta* **176**, 527–532 (1988).
10. Keeley, J. E. CAM photosynthesis in submerged aquatic plants. *Bot. Rev.* **64**, 121–175 (1998).
11. Keeley, J. E., Osmond, C. B. & Raven, J. A. *Stylites*, a vascular land plant without stomata absorbs CO<sub>2</sub> via its roots. *Nature* **310**, 694–695 (1984).
12. Hibberd, J. M. et al. Localization of photosynthetic metabolism in the parasitic angiosperm *Cuscuta reflexa*. *Planta* **205**, 506–513 (1998).
13. Esau, K. *Plant Anatomy* 2nd edn (John Wiley, New York, 1965).
14. Kinsman, E. A. & Pyke, K. A. Bundle sheath cells and cell-specific plastid development in *Arabidopsis* leaves. *Development* **125**, 1815–1822 (1998).
15. Nilsen, E. T. in *Plant Stems* (ed. Gartner, B. L.) 223–240 (Academic, San Diego, 1995).
16. Raven, J. A. Long-term functioning of enucleate sieve elements: possible mechanisms of damage avoidance and damage repair. *Plant Cell Environ.* **14**, 139–146 (1991).
17. Gerendas, J. & Schurr, U. Physicochemical aspects of ion relations and pH regulation in plants—a quantitative approach. *J. Exp. Bot.* **50**, 1101–1114 (1999).
18. Cramer, M. D. & Richards, M. B. The effect of rhizosphere dissolved inorganic carbon on gas exchange characteristics and growth rates of tomato seedlings. *J. Exp. Bot.* **50**, 79–87 (1999).
19. Cramer, M. D., Gao, Z. F. & Lips, S. H. The influence of dissolved inorganic carbon in the rhizosphere on carbon and nitrogen metabolism in salinity treated tomato plants. *New Phytol.* **142**, 441–450 (1999).
20. Vuorinen, A. R., Rossi, P. & Vapaavuori, E. M. Combined effect of inorganic carbon and different nitrogen sources in the growth media on biomass production and nitrogen uptake in young willow and birch plants. *J. Plant Physiol.* **147**, 236–242 (1995).
21. Pate, J. S. in *Encyclopedia of Plant Physiology* Vol. 1 (eds Zimmerman, M. H. & Milburn, J. A.) 451–473 (Springer, Heidelberg, 1975).
22. Raven, J. A. & Smith, F. A. Nitrogen assimilation and transport in vascular land plants in relation to intracellular pH regulation. *New Phytol.* **76**, 415–431 (1976).
23. Ben Zioni, A., Vaadia, Y. & Lips, S. H. Nitrate uptake by roots as regulated by nitrate reduction products of the shoot. *Physiol. Plant.* **24**, 288–290 (1971).
24. Hibberd, J. M., Quick, W. P., Press, M. C., Scholes, J. D. & Jeschke, W. D. Solute fluxes from tobacco to the parasitic angiosperm *Orobancha cernua* and the influence of infection on host carbon and nitrogen relations. *Plant Cell Environ.* **22**, 937–947 (1999).
25. Ashton, A. R., Burnell, J. N., Furbank, R. T., Jenkins, C. L. D. & Hatch, M. D. in *Methods in Plant Biochemistry*, Vol. 3 (ed. Lea, P. J.) 39–72 (Academic, San Diego, 1990).
26. Lea, P. J. & Leegood, R. C. *Plant Biochemistry and Molecular Biology* (Wiley, Chichester, 1999).
27. Schaaf, J., Walter, M. H. & Hess, D. Primary metabolism in plant defence. *Plant Physiol.* **108**, 949–960 (1995).
28. Gao, Z., Sagi, M. & Lips, M. Assimilate allocation priority as affected by nitrogen compounds in the xylem sap of tomato. *Plant Physiol. Biochem.* **34**, 807–815 (1996).
29. Thomas, J. C., De Armond, R. L. & Bohnert, H. J. Influence of NaCl on growth, proline and phosphoenolpyruvate carboxylase levels in *Mesembryanthemum crystallinum* suspension cultures. *Plant Physiol.* **98**, 626–631 (1992).
30. Walker, R. P., Trevanion, S. J. & Leegood, R. C. Phosphoenolpyruvate carboxykinase from higher plants: Purification from cucumber and evidence of rapid proteolytic cleavage in extracts from a range of plant tissues. *Planta* **196**, 58–63 (1995).

## Acknowledgements

We thank J. C. Gray and W. D. Jeschke for discussions. J.M.H. thanks the BBSRC for a Sir David Phillips Research Fellowship.

## Competing interests statement

The authors declare that they have no competing financial interests.

Correspondence and requests for materials should be addressed to J.M.H. (e-mail: julian.hibberd@plantsci.cam.ac.uk).

# Anaerobic microbial metabolism can proceed close to thermodynamic limits

Bradley E. Jackson & Michael J. McInerney

Department of Botany and Microbiology, University of Oklahoma, 770 Van Vleet Oval, Norman, Oklahoma 73019-2045, USA

Many fermentative bacteria obtain energy for growth by reactions in which the change in free energy ( $\Delta G'$ ) is less than that needed to synthesize ATP<sup>1–4</sup>. These bacteria couple substrate metabolism directly to ATP synthesis, however, by classical phosphoryl transfer reactions<sup>4,5</sup>. An explanation for the energy economy of these organisms is that biological systems conserve energy in discrete

amounts<sup>3,4</sup>, with a minimum, biochemically convertible energy value of about  $-20 \text{ kJ mol}^{-1}$  (refs 1–3). This concept predicts that anaerobic substrate decay ceases before the minimum free energy value is reached, and several studies support this prediction<sup>1,6–9</sup>. Here we show that metabolism by syntrophic associations, in which the degradation of a substrate by one species is thermodynamically possible only through removal of the end product by another species<sup>1</sup>, can occur at values close to thermodynamic equilibrium ( $\Delta G' \approx 0 \text{ kJ mol}^{-1}$ ). The free energy remaining when substrate metabolism halts is not constant; it depends on the terminal electron-accepting reaction and the amount of energy required for substrate activation. Syntrophic associations metabolize near thermodynamic equilibrium, indicating that bacteria operate extremely efficient catabolic systems.

Anaerobic bacteria capable of syntrophic metabolism thrive in environmental niches where amounts of free energy are at a minimum<sup>1</sup>, and therefore represent ideal microbial systems for testing bioenergetic concepts. In syntrophic associations, the degradation of a substrate by one species is made thermodynamically possible through the removal of end products by another species (ref. 1; and Table 1). Syntrophic interactions are widespread, occurring in both manmade and natural environments such as sewage digesters, municipal landfills, hydrocarbon-contaminated soils, freshwater sediments and waterlogged soils<sup>1,10–12</sup>. The ubiquity of such interactions emphasizes the fact that, in most environments, metabolic cooperation among microbial species is required for the complete destruction of organic matter<sup>1,12</sup>.

We observed previously that syntrophic cultures only partially degrade their substrate, stopping at a threshold concentration<sup>7,13</sup>. The resulting substrate threshold was large in some cases, up to 1.5 mM, and remained unchanged for up to 360 days of incubation<sup>13</sup>. Experiments have shown that nutritional limitation, loss of metabolic activity, inhibition by high hydrogen or formate concentrations, kinetic inhibition and toxicity from build-up of the undissociated form of acetate are not the cause of this threshold<sup>7,8,13</sup>. The substrate threshold concentration was, however, influenced by the accumulation of end product (specifically acetate). We concluded that the extent of substrate degradation was controlled by a thermodynamic, mass-action effect<sup>7,13</sup>.

By manipulating substrate degradation and threshold formation, we tested the hypothesis that a minimum quantum of free energy is needed to sustain microbial metabolism. On the basis of universal biological energy quantum theory<sup>1–3</sup>, we posited the following predictions: first, substrate degradation will cease at a threshold concentration that corresponds to a critical free energy value ( $\Delta G'_{\text{crit}}$ ) independent of the species or substrate involved; second, the  $\Delta G'_{\text{crit}}$  value at threshold will be constant (not appreciably lower or higher than  $-20 \text{ kJ mol}^{-1}$ ); and third, the  $\Delta G'_{\text{crit}}$  will not be affected by different substrates or terminal electron-accepting schemes.

Benzoate and butyrate were used as model substrates, because each of these is a key intermediate in the degradation of diverse organic compounds<sup>3,12,14</sup>. Each compound was added to defined cocultures containing a syntrophically oxidizing bacterium and a hydrogen-consuming partner. Table 2 shows the results of butyrate degradation by a typical *Syntrophus aciditrophicus* coculture grown under sulphate-reducing conditions (with *Desulfovibrio* sp. strain G11) when stressed with different concentrations of acetate. Roughly 2.5 mM butyrate was degraded incompletely to a threshold concentration that ranged from 5 to 250  $\mu\text{M}$ , depending on the final concentration of acetate. Hydrogen partial pressures were low, ranging from  $0.22 \pm 0.06$  to  $0.31 \pm 0.05 \text{ Pa}$ , and formate was not detected (detection limit of 1  $\mu\text{M}$ ).

The extent of butyrate degradation depended on the amount of acetate in the system, which is consistent with the interpretation that the accumulation of end products thermodynamically controls the extent of substrate degradation. Even though the final butyrate